Leaf shape and size variation in bur oaks: An empirical study and simulation of sampling strategies

Sara C. Desmond[1,*], Mira Garner[1,2], Seamus Flannery[1,3,4], Alan T. Whittemore[5] and Andrew L. Hipp[1,5,6,*]

[1] The Morton Arboretum, Center for Tree Science, 4100 Illinois Route 53, Lisle, IL 60532, USA

[2] Current address: The University of British Columbia, UBC Faculty of Forestry, Vancouver, BC Canada V6T 1Z4

[3] The University of Chicago Laboratory Schools, 1362 East 59th St., Chicago, IL 60637, USA

[4] Current address: Haverford College, 370 Lancaster Avenue, Haverford, PA 19041, USA

[5] U.S. National Arboretum, 3501 New York Ave NE, Washington, DC 20002, USA

[6] The Field Museum, 1400 S Lake Shore Drive, Chicago, IL 60605, USA

[7] Author for correspondence (email: ahipp@mortonarb.org)

[*] These authors contributed equally to writing and data analysis for this paper.

ABSTRACT

PREMISE: Oaks are notoriously variable in leaf morphology, but little is known regarding the partial contributions of climate, population, latitude, and individual tree to total variation in leaf morphology. This study examines the contributions of within-tree, among-tree, and among-site variation to the total variation in leaf morphology in bur oak (*Quercus macrocarpa*), one of North America's most geographically widespread oak species.

METHODS: Samples were collected from four sites each at northern, central, and southern latitudes of the bur oak range. Ten leaf size traits were measured, and variance in these traits and eight ratios was partitioned into tree, population, and latitude components. We then parameterized a series of leaf collections simulations using empirical covariance among leaves on trees and trees at sites.

KEY RESULTS: Leaf size measurements were highly responsive to latitude. Site contributed more than tree to total variation in leaf morphology. Simulations suggest that power to detect among-site variance in leaf morphology can be estimated most efficiently with increases in either leaves per tree (10-11 leaves from each of 5 trees) or trees per site (5 leaves from each of 10+ trees).

CONCLUSIONS: Our study demonstrates the utility of both simulating sampling and controlling for variance in sampling for leaf morphology, whether the questions being addressed are ecological, evolutionary, or taxonomic. Simulation code is provided to help researchers plan sampling strategies to maximize the ability to detect among-site variance in leaf morphology.

Keywords: climate; Fagaceae; latitude; leaf morphology; leaf size; *Quercus macrocarpa*; sampling simulation

Running head: Leaf morphological variation in bur oak

Manuscript received _____; revision accepted _____.

INTRODUCTION

Leaf morphology variation strongly influences species' ability to compete and survive in different environments (Givnish, 1987). It has long been recognized that there is a correlation between temperature and the proportion of species exhibiting leaf dissection and toothing, and for more than a century this correlation has been used to model temperature changes in paleobotanical studies (Bailey and Sinnott, 1915, 1916; Greenwood et al., 2004; Royer and Wilf, 2006). Leaf size similarly has a well demonstrated correlation with temperature and resource availability (Bragg and Westoby, 2002; Peppe et al., 2011; McKee and Royer, 2017; Wright et al., 2017; Li et al., 2020), and traits such as compounding and phyllotaxy, base and apex morphology, leaf shape, and epidermal pigmentation vary along gradients of light availability, nutrient availability, soil moisture, temperature, or combinations of these (Givnish, 1987; Schmerler et al., 2012). In a global field study from 92 sites (Peppe et al., 2011), multiple regressions of climate (both precipitation and temperature) on leaf area, tooth number, and percent of species at the site with toothing showed relatively high predictive ability, inferred from the low standard error of the models (±4℃). However, while the sign of this correlation—more toothing and lobing in cooler areas—is convergent across clades and geographic regions, the slope of the relationship between climate and leaf morphology varies among species (McKee et al., 2019), geographic regions (Greenwood et al., 2004; Aizen and Ezcurra, 2008), and phylogenetic lineages (Little et al., 2010; Burnham and Tonkovich, 2011; Walls, 2011).

Many of these traits vary both among and within species, and correlations between community-weighted mean trait values at the site level are mirrored within species on short time scales, with toothing and leaf lobing correlated with cooler temperatures in most species studied as well as across communities (McKee and Royer, 2017; McKee et al., 2019). Moreover, the morphology of leaves can vary highly within communities (Givnish, 1987). Within forest trees in

particular, variation due to position on the tree (Blue and Jensen, 1988; McCarthy and Mason-Gamer, 2019), light availability (Abrams and Kubiske, 1990; Ducrey, 1992), drought (Abrams, 1994; Abrams et al., 1994) as well as genetic differences among trees within species (Abrams, 1994; Ramírez-Valiente et al., 2017) all contribute to variation in leaf shape and size. Moreover, while sampling of a small number of leaves per population has been argued to be sufficient for detecting site level patterns in climate based in paleobotanical studies (Royer et al., 2005; Peppe et al., 2011), the relative contribution of within-tree, among-tree within-population, and among-population variation to total morphological variation is not clear in many tree species, leading to observations for example that variation among leaves on a single tree is sometimes as great as the variation observed among named species (e.g., McCarthy and Mason-Gamer, 2019).

Oaks have long been noted for their particularly variable morphology at all levels (among leaves on a single tree, among trees of a single population, and among populations of a single species). Detailed studies in oaks have utilized either linear measurements (Baranski, 1975; Blue and Jensen, 1988; Bruschi et al., 2003) or landmark approaches (Jensen, 1990). Both approaches have demonstrated that while variation among positions within a tree in both leaf shape and size may exceed variation among sites, overall variance is generally greater among sites. These papers have highlighted that studies investigating among-population divergence patterns can minimize within-individual morphological variance by holding sampling season and leaf position on the tree constant (i.e., high or low on the tree and disposed toward the edges or inside of the canopy) (Sokal et al., 1986; Blue and Jensen, 1988; Bruschi et al., 2003). Understanding these sources of variance in leaf shape and size is foundational to understanding how introgression, adaptation, and neutral variation influence leaf morphology both among and within species (Jensen et al., 1984; Howard et al., 1997; Kremer et al., 2002; González-Rodríguez et al., 2004;

González-Rodríguez and Oyama, 2005) and the balancing act that trees face in maximizing photosynthetic efficiency while minimizing the risks of drought, freezing, herbivory and other stresses (Wright et al., 2004). However, it is not clear what sampling strategy (leaves per individual, individuals per population) is most efficient for estimating among-population differences in leaf size and shape. Whereas simple simulation tools exist for planning sampling strategies for population genetics (Hoban et al., 2013; Hoban, 2014) and conservation of genetic diversity (Hoban, 2019; Hoban et al., 2020), morphological sampling strategies that take into account covariance among leaves on a tree, among trees in a population, and among traits measured are lacking. Given that resources for sampling are limited, tools to help plan sampling strategies would make it possible to answer questions more definitively with the same amount of field work.

We sampled leaves across a broad geographic range of bur oak (*Quercus macrocarpa* L.), one of North America's most geographically widespread oak species, which ranges from Manitoba to the Gulf of Mexico (Fig. 1) to (1) quantify the relative contributions of within-tree, among-tree, and among-site variation to the total variation in leaf morphology in bur oak; (2) use this information to simulate how much sampling is required to detect among-site differences in leaf morphology; and (3) test the support for our observations in field and herbarium that leaf size and leaf-lobing increase from north to south in bur oak. Bur oak serves as an excellent model species for this study because it has exceptionally high morphological variation (Hamerlynck and Knapp, 1994; Koenig et al., 2009) and an extensive distribution, ranging from Manitoba to the Gulf of Mexico (Little, 1971; Stein et al., 2003). The species also exhibits high within-population molecular genetic variation (Schnabel and Hamrick, 1990; Garner et al., 2019; Hipp et al., 2019), suggesting that an investigation of the leaf morphological variation among vs

within sites is appropriate as a precursor to future studies of what environmental factors contribute to morphological variation in bur oak leaves.

MATERIALS AND METHODS

***Collections and site attributes*—**During the summer and fall of 2017, samples were collected from four sites each at northern, central, and southern latitudes of the bur oak range (Fig. 1). Sites were selected in conjunction with sampling for ongoing population genetic studies of *Quercus macrocarpa* (Garner et al., 2019; Hipp et al., 2019) with the criteria that (1) preliminary collections suggested they would have numerous bur oaks, and (2) additional white oaks were present at the site or nearby. Most were forested, but some (e.g. The Morton Arboretum, Prairie Moon Nursery) were savannas. The northern sites sampled were located in Manitoba (Assiniboine Park, Whiteshell Provincial Park, and Spruce Woods Provincial Park) and Minnesota (The University of Minnesota – Twin Cities). The central sites sampled were located in Illinois (The Morton Arboretum), Indiana (Burr Oak Woods), Iowa (Cherokee Park Trail), and Minnesota (Prairie Moon Nursery). The southern sites sampled were located in Oklahoma (Tallgrass Prairie Preserve, Mohawk Park, Red Rock Canyon State Park) and Missouri (Buttin Rock Access). Trees selected at each site were mature, full-size trees; where possible, trees at a given site were located a minimum of 100 feet from each other. For each site, latitude and longitude were recorded to a precision of 5 decimal places (Table 1). We extracted 19 bioclim variables from the WorldClim database (resolution = 1 km^2) and linked them to our dataset in R v. 3.4.4 (R Core Team, 2018) using raster v 2.6-7 (Hijmans, 2017) and sp_1.4-2 (Pebesma and Bivand, 2005; Bivand et al., 2013) packages. The map of collection sites was made using maps 3.3.0 (Becker et al., 2018).

Three bur oak trees were sampled from each site using a pole pruner at two or four meters in height, based on tree height. For each sample, a terminal branch was cut down from each of the cardinal directions (N, S, E, W), determined using a compass. Only outermost branches were sampled. Two endmost leaves were removed from each branch and immediately pressed, for a total of 8 leaves per individual, 272 leaves overall. If the endmost leaves were highly damaged, the next leaves in from the end were selected. Leaves that were highly misshapen or broken were excluded from analyses (see 'use' field in dataset archived in GitHub, which indicates which leaves were excluded from analysis). Leaves were dried in a standard herbarium drier prior to measuring, then redried at 49° C for a minimum of 48 hours and weighed on a PB303 Delta Range scale to obtain dry mass.

***Morphological Measurements*—**Ten size measurements (mm) were made on each leaf using ImageJ (Schneider et al., 2012): blade length (bladeL), blade width (bladeW), width of blade between deepest pair of sinuses (sinusMinW), petiole length (petioleL), petiole width (petioleW), length of lamina from base to widest point (bladeLtoWidestPoint), width of blade between pair of sinuses just above the deepest pair (sinusNextW), total length (BL.PL), leaf base angle (bladeBaseAngle), and leaf area (Area) (Table 2, Fig. 2). Seven ratios were also calculated from these measurements to distinguish leaf shape from leaf size (González-Rodríguez and Oyama, 2005): petioleL / BL.PL (PL.TL); sinusMinL / sinusNextL (SinusRatio); bladeL / bladeW (BL.BW); petioleL / petioleW (PL.PW); BL.BW / PL.PW (BL.BW.over.PL.PW); bladeL / bladeLtoWidestPoint (BL.BLWP); lobedness, calculated as blade width between the deepest sinuses divided by total blade width, abbreviated (sinus.v.width); and specific leaf area

(SLA), calculated as leaf blade area / leaf blade mass (Table 2). A panel of significant regressions was created using the R core functions and gridExtra 2.3 (Auguie, 2017).

To investigate lobedness using more complex morphometric approaches, black and white silhouettes of each leaf image were created using ImageJ and converted into jpeg files, with petioles whited out manually. The jpeg files were then imported into R and converted into outlines using the R package Momocs v 1.3.2 (Bonhomme et al., 2014). An additional set of 40 leaves that did not import well into Momocs or had leaf outlines that did not impair manual measurements but that were badly non-representative of typical leaf form were deleted at this stage (see scripts 05a and 05b in the GitHub repository for enumeration of these). We initially investigated shape variation using elliptical Fourier analysis (EFA), which generates shape-representative variables that are independent of size (Crampton, 1995) and is well suited to comparing complex outlines that vary in shape and lobedness (Tracey et al., 2006). For these analyses, we normalized the outlines using four landmarks placed on the top, bottom, left, and right of each outline and analyzed the leaf outlines using 17 harmonics (the default setting).

We also used Momocs to measure circularity (as the square of perimeter over the area) (Rosin, 2005) and Haralick's circularity (as the mean distance from the leaf centroid to the perimeter pixels divided by the standard deviation of those distances) (Haralick, 1974). Haralick's circularity is less sensitive to shape raggedness than the standard measure of circularity and increases with increasing circularity; standard circularity decreases with increasing circularity. We aggregated both circularity measures to individual and then individuals to site to examine site-level effects of latitude on leaf circularity using simple least-squares regressions.

Statistical Analysis—*Linear Regressions and ANOVA***—**All statistical analyses were conducted in R. Seventeen least squares were performed on all leaf linear measurements using the lm function to assess which leaf traits were most responsive to latitude at the site level, aggregating leaf traits first to tree, then tree mean trait values to site. An additional regression was performed of Haralick circularity on latitude, at the site level. Data were visualized using ggplot2 3.3.2 (Wickham, 2009). In addition to simple regressions, we corrected for size by conducting multiple regressions for all of our leaf traits using the lm function and including blade length (bladeL) as a covariate. We used data scaled to a mean of zero and unit variance.

We performed a principal component analysis (PCA_{MORPH}) on all scalar measurements and ratios using the prcomp function. The point MN-MG788 was removed prior to analysis because it significantly skewed the ordination. Two-dimensional nonmetric multidimensional scaling on a Euclidean distance matrix based on principal component axes was used to visualize the data. The scaling type was 'centering' with PC rotation. We used the ordiellipse function in vegan 2.4-5 (Oksanen et al., 2017) to plot bounding ellipses on our ordination.

Two-way ANOVA was used to assess the relative contributions of site and tree to the total variation in bladeL, SLA, $PC1_{MORPH}$ and $PC2_{MORPH}$. Principal components one and two were extracted from the principal component analysis mentioned above and attached to our original dataset. ANOVA was conducted on the linear model of bladeL, SLA, $PC1_{MORPH}$, and $PC2_{MORPH}$ regressed against site and tree. We chose $PC1_{MORPH}$ and $PC2_{MORPH}$ for this analysis because together they accounted for 52.5% of the variance.

Simulations of sampling strategies—We assessed the effectiveness of alternative sampling scenarios to distinguish differences among populations by using our estimates of

variation to generate simulated morphological datasets for 20 populations that ranged from three to 12 trees per site and three to 12 leaves per tree, a total of 100 sampling strategies. For each strategy, we simulated 100 replicate datasets of all ten direct morphological measurements using a hierarchical simulation strategy, using the data we collected to parameterize the simulation. For each replicate, site-level means for all 10 traits were drawn from the multivariate normal distribution with trait means and covariance $\mathbf{C}_{site}$ estimated from observed site means for all traits; $\mathbf{C}_{site}$ is thus based on variance within and covariance among traits that we observed, averaged for each site. Tree-level means were then drawn from the multivariate normal distribution with the simulated site-level means and the covariance matrix $\mathbf{C}_{tree}$ estimated from tree means at each site and averaged across sites: tree-level means were thus assumed to have a constant variance and covariance among sites. Finally, individual leaf measurements for each tree were drawn from the multivariate normal distribution with means from the second simulation stage and covariance matrix $\mathbf{C}_{leaf}$ estimated from the leaf measurements for each tree separately, then averaged across trees.

The resulting 100,000 data matrices ranged from 180 to 2,880 simulated leaves, with trait covariance and variance among leaves within trees, among trees within populations, and among populations modeled according the measurements we made for this project. Because leaf size showed particularly strong variation among populations, we utilized ANOVA of bladeL on site + tree, combined with Tukey's Honest Significant Different (HSD) method to assess the number of populations that could be differentiated from one another in each simulated data matrix. The number of letters needed for a compact letter display using Tukey's HSD at $\alpha = 0.05$ was used as a proxy for the number of groups that could be distinguished for each simulated dataset. Both the average number of groups distinguished for each simulated dataset and the percent of

simulations that distinguish at least 50% of populations (10 / 20) are reported as estimates of statistical power. All simulations were conducted in R using mvtnorm v 1.0-11 (Genz and Bretz, 2009; Genz et al., 2019) (Genz et al. 2017), and code for performing simulations is archived in GitHub and Zenodo (https://github.com/andrew-hipp/oak-morph-2020; https://doi.org/10.5281/zenodo.4213821). The simulation code can be installed as package 'traitsPopSim' from GitHub (https://github.com/andrew-hipp/traitsPopSim) and run using multivariate traits collected in a similarly structured design (measurements nested within individuals nested within sites; sample data included in the package are from the current study).

RESULTS

***Analysis of empirical data*—**Among the size characters, bladeL, bladeW, BL.PL, petioleW, and Area all showed significant variation in response to latitude (Table 3, Fig. 3). Petiole width was the size trait that was the most significant ($P < 0.001$). Petiole length, sinusMinL, sinusNextL, and blade base angle were not significantly predicted by latitude (Table 3). Two ratios were significantly correlated with latitude: SLA ($r^2 = 0.466$, $P = 0.015$) and the ratio of sinus depth to leaf width (sinus.v.width, a proxy for lobedness; $r^2 = 0.415$, $P = 0.024$) (Table 3). In regressions controlling for size by including bladeL as a covariate, sinusNextL ($P = 0.021$), petioleW ($P = 0.017$), bladeL ($P = 0.012$) and SLA ($P = 0.011$) were the only traits significantly affected by latitude alone (Table 3; Fig. 3). Regressions of all traits measured, significant or not, are presented in the supplement (Supplemental Fig. S1). Standard circularity (perimeter squared over area) was strongly affected by latitude ($r^2 = 0.506$, $P = 0.0043$; Fig. 4), Haralick circularity (mean distance from leaf centroid to boundary pixels over the standard deviation of these

distances) was weakly predicted by latitude ($r2$ = 0.259, P = 0.063l; Fig. 4). Under both measures, southern leaves exhibited stronger lobing, northern leaves exhibited greater circularity.

PCA on the EFA yielded very high loading on PC1 (58%), very low on PC2 (8%), and a strong curvilinear relationship between PC1 and PC2 (Supplemental Fig. S2). This non-independence between PC1 and PC2 can arise because variation is broad, such that the ends of the PC cloud have little in common, or because the variation is dominated by a single variable (Minchin, 1987). In our study, PC1 was dominated by size (Pearson's product moment [r] = 0.251 for blade width, 0.227 for blade area) and latitude (r = –0.213), and PC2 was more strongly associated with shape (r = 0.395 for the ratio of blade length to blade width, –0.375 for width of the sinus distal to the deepest sinus, 0.348 for the ratio of the width of the blade in the deepest sinus width of the blade in the second-deepest sinus), and to a lesser extent leaf blade width (r = –0.240).

The effects of site and tree on bladeL, SLA, and the first two axes of the morphological (non-EFA) ordination (Supplemental Fig. S3) were significant based on ANOVA (P << 0.001; Table 4). Although site and tree both had significant effects, site contributed more than tree to the total variation in leaf morphology (F-values for site range from 30.38–41.76, while F-values for tree range from 5.83–12.4). Mean annual temperature among our sites ranged from 2.1–15.3°C, and mean annual precipitation from 460 – 1121 mm. On average, leaf bladeL averaged 34.0 mm shorter and SLA 50.39 mm^2/g greater for each increase 10 degrees in latitude (northward).

Regressions of individual traits on site-level temperature and moisture conditions inferred from BioClim closely matched regressions of those same traits on latitude. The latitudinal gradient in our study correlated tightly with climate: increases in latitude entail decreases in

mean annual precipitation (Bio12; R^2 = 0.6803, p < 0.01) and temperature (Bio1; r^2= 0.99, p << 0.01), and an increase in temperature seasonality (Bio4; R^2 = 0.97, p << 0.01) (Fig. 5). As a consequence, climate is not considered further in this study, but only latitude.

***Analysis of simulated data*—**The mean number of groups distinguished in our simulations ranged from 5.49 to 10.41, and the probability of distinguishing 50% (10 / 20) of the populations based on blade length ranged from 0.01 to 0.71 (Fig. 6). The sampling strategy we implemented for this study, 3 trees per site, 8 leaves per tree, had a power of only 38% to identify a number of groups equal to 50% of the sites sampled. Increasing power to at least 50% would entail increasing sampling to 11–12 leaves from each of 5 trees, 5 leaves from each of 10–11 trees, or any of a number of scenarios intermediate between these extremes.

DISCUSSION

Our study has three important findings. First, among-tree and among-site variation contribute significantly to leaf shape and size variation in bur oaks. Consequently, within-individual and within-population sampling are both important components of a sampling strategy aimed at characterizing among-population variation in oak morphology. This complements observations of high variance in temperate tree leaf morphology (Bruschi et al., 2003; Apostol et al., 2017; McCarthy and Mason-Gamer, 2019), demonstrating that among-site variation contributes most strongly to total leaf variation, but that within-site and within-tree sampling are important to detecting among-site variation in leaf shape and size. Second, we implement a general parametric simulation method and use it to demonstrate that our sampling strategy, which included 8 leaves from different positions on each of 3 trees per site, was not optimal for

296 resolving among-site variation, even if it was sufficient to demonstrate the relationship between
297 morphology and latitudinal gradients. This simulation approach and the package provided
298 (traitsPopSim) can serve as tools to guide morphological sampling in similar hierarchical studies,
299 where sites are composed of multiple individuals and individuals are each represented by
300 multiple measurements. Finally, our study demonstrates that leaf size and lobing decrease from
301 south to north in bur oak, while specific leaf area increases. In cross-species comparisons, leaf
302 size and SLA generally covary, suggesting that adaptive leaf variation in bur oak may rest in part
303 on a tradeoff between leaf size and lobing. Our study of one of North America's most
304 widespread oak species is thus a jumping-off point for understanding adaptive leaf variation
305 across the oaks of the Americas.
306
307 ***Leaf size and shape variance are influenced by population and individual*—**Our results
308 show that among-site variance for all traits investigated ($F_{11,236}$ = 30.38–41.76) contributes more
309 to total variance in leaf morphology than among-tree variance ($F_{11,236}$ = 5.83–12.42), though both
310 variance components are significant ($P << 0.001$; Table 4). This ability to distinguish among
311 sites is important in relating leaf variation to latitude or climatic predictors and measuring the
312 slope of the relationship resulting from selective pressures along climatic gradients (Wright et
313 al., 2004). Moreover, our results demonstrate that sampling three trees per site, and eight leaves
314 per tree is sufficient to correlate shape and size to latitude and climate. However, while among-
315 site variance is higher than among-tree variance within sites (Table 4), the variance we observe
316 among leaves within a single tree is still quite high. A previous study (Bruschi et al., 2003) found
317 that among-leaf morphological variance on a tree is higher than among-tree variance for most
318 traits investigated, and that this was in accord with findings from earlier work (Baranski, 1975;

Blue and Jensen, 1988). However, in Bruschi (2003), leaves were sampled from both inner and outer positions on the branch to maximize variance. In our study, we deliberately minimized this source of variance by sampling leaves at a relatively constant height and all from the outer branch position, and we further selected the endmost leaves from each branch sampled.

***Simulating sampling strategies*—**The simulations we conducted of alternative sampling strategies suggests the strategy we selected of three trees per site and eight leaves per tree has only a 38% probability of distinguishing 50% of 20 populations drawn at random from distributions we observed. It may well be that our difficulty relating shape to climate is due to a lack of sampling within sites and trees. Based on the variance observed in leaf length alone, achieving a 50% probability of distinguishing 50% of populations would require 11–12 leaves from each of 5 trees per site, 5–6 leaves from each of 11–12 trees per site, or something in between (Fig. 6).

Our simulations suggest two recommendations for others conducting similar studies. First, researchers are recommended to minimize the high within-individual variance observed in previous studies (Blue and Jensen, 1988; Bruschi et al., 2003; McCarthy and Mason-Gamer, 2019) by sampling leaves of a common age / developmental stage, in the same position on the twig, and from twigs with comparable positions on the plants. Second, simulating alternative sampling strategies will help maximize the ability to distinguish among populations, given limited time and resources. Researchers can use preliminary data to simulate alternative sampling strategies and estimate their power will be to distinguish populations under different scenarios. The tools we developed for this study require only a matrix of traits and assignment of those traits to populations and individuals to perform the simulations we describe above. We expect that their use will facilitate planning of sampling designs for similar projects.

342 ***Leaf size, lobing, and SLA are predicted by latitude—*** The measurements for each of our
343 leaves were well predicted by their latitude of origin: leaves were thicker, larger, and had deeper
344 lobes at southern latitudes, where leaves are exposed to warmer temperatures and higher
345 precipitation, and have longer growing seasons; and leaves were smaller, thinner, and had
346 shallower lobes at northern latitudes, where cold temperatures reduce water stress. This is in line
347 with previous studies demonstrating that leaf area covaries positively with temperature (Moles et
348 al., 2014; Wright et al., 2017) while SLA covaries negatively (Moles et al., 2014), and that leaf
349 circularity tends to increase in northern or cooler environments (Halloy and Mark, 1996;
350 Schmerler et al., 2012). Our results also parallel previous work in *Quercus ilex*, which exhibited
351 a similar leaf size gradient from north to south in the western Mediterranean basin, where
352 southern regions were likewise warmer and had higher amounts of precipitation than northern
353 regions (García□Nogales et al., 2016).
354 Our findings suggest a possible compensatory relationship between larger size and lobing
355 in bur oak. Community-level studies tend to show a higher frequency of lobed leaves in cooler
356 temperatures (Royer et al., 2005). These responses are individualistic, however, and among-
357 population responses in some species show no response or greater lobing in warmer temperatures
358 (Royer et al., 2008; McKee and Royer, 2017; McKee et al., 2019). Leaves that are deeply lobed
359 may be better adapted to warmer climates, because deeply lobed and narrow leaves have a
360 thinner leaf boundary layer, facilitating more rapid cooling (Givnish, 1987; McDonald et al.,
361 2003). In our study, the ratio of sinus depth to leaf width (sinus.v.width) shows a weak negative
362 correlation with latitude (b = 0.013, P = 0.024), but this result is strongly affected by one site,
363 Red Rock Canyon, which had an exceptionally low value. When this outlier is removed, the
364 correlation is no longer significant (b = 0.007, P = 0.054). In multiple regressions with scaled

data and bladeL as a covariate, however, depth of the sinus immediately above the deepest sinus (sinusNextL) was significantly influenced by latitude (b = 0.893, P = 0.021), even with the outlier removed (b = 0.926, P = 0.023). Our whole-leaf estimates of shape (circularity and Haralick circularity) similarly both showed increased circularity northward, but their sensitivity to the latitudinal gradient is different. This may be a consequence to the relative insensitivity of Haralick circularity to leaf toothing (Haralick, 1974), which manifests in bur oak as differences in crenulation. We did not quantify this effect directly, but leave it to future studies.

The hypothesis that leaf lobing increases southward in response to increased water stress is supported by the specific leaf area (SLA) data. With leaf length as a covariate, SLA increases northward (b = 0.987, P = 0.011), even as leaf size decreases. Leaves that are low in SLA have higher water use efficiency (Mooney and Dunn, 1970; Marron et al., 2003; Liu et al., 2017) and have been shown to vary within oaks according to water stress (Ramírez-Valiente and Cavender-Bares, 2017; Ramírez-Valiente et al., 2017). This corresponds with our finding that bur oak leaves at southern sites, where trees are exposed to warmer temperatures and are likely more water-stressed, had significantly lower SLA than leaves collected at northern sites. However, leaf area in cross-species oak comparisons covaries with SLA (Ramírez□Valiente et al., 2020), and leaf area and SLA both decrease on average with increased water stress in cross-species comparisons (Kaproth and Cavender-Bares, 2016; Ramírez□Valiente et al., 2020). Our finding of larger leaf areas with lower SLA in bur oak, but with an increase in lobing, suggests that leaf lobing may compensate for increased size in areas with great water stress.

The immense success of oaks (*Quercus*) in the Americas (Rodríguez-Correa et al., 2015; Hipp et al., 2018; Cavender-Bares, 2019) has been attributed in part to oaks' ability to cross the temperate-tropical divide. Bur oak is exceptional in its climatic range, extending from near the

388 boreal zone in the north to the great plains and the humid subtropics. Our finding that leaf lobing,
389 SLA, and leaf size compensate for one another along climatic gradients in bur oak may be
390 echoed in other species. The work presented here consequently has the potential to inform
391 studies of adaptive variation across oaks and temperate tree species more generally.
392
393 **ACKNOWLEDGMENTS**
394 This study was funded by The Morton Arboretum Center for Tree Science and USDA
395 Project 8020-21000-070-03S, a non-assistance cooperative agreement between U.S. National
396 Arboretum and The Morton Arboretum. We would like to thank Marlene Hahn for assisting with
397 curation of herbarium and leaf samples and Matthew Kaproth for advice on measurement of
398 SLA. Ricardo Kriebel provided particularly detailed advice on morphometric analysis, including
399 code to assist in generating landmarks and excellent feedback on interpretation of our results;
400 and Associate Editor Dylan Schwilk, with an anonymous reviewer and Kriebel, provided
401 editorial feedback that substantially improved the manuscript.
402
403 **AUTHOR CONTRIBUTIONS**
404 A.L.H., A.T.W. and S.C.D. conceptualized and designed the project. S.C.D., M.G., and
405 S.F. collected specimens and data. S.C.D. and A.L.H. conducted data analyses. S.C.D. wrote the
406 first draft of the manuscript, and A.L.H. revised the manuscript in response to reviewers. A.L.H.
407 coded and analyzed simulations and contributed to data analysis. All authors contributed to
408 writing and revisions; A.L.H. and S.C.D. contributed equally to analysis and writing.
409
410 **DATA ACCESSIBILITY**

411 Data and scripts used to conduct the statistical analysis are archived in GitHub
412 (https://github.com/andrew-hipp/oak-morph-2020) and released through Zenodo
413 (https://doi.org/10.5281/zenodo.4213821). Supplemental figures are available in the GitHub
414 repository and in the online Supplement.

415 **REFERENCES CITED**

416 Abrams, M. D. 1994. Genotypic and phenotypic variation as stress adaptations in temperate
417 tree species: a review of several case studies. *Tree Physiology* 14: 833–842.

418 Abrams, M. D., and M. E. Kubiske. 1990. Leaf structural characteristics of 31 hardwood and
419 conifer tree species in central Wisconsin: Influence of light regime and shade-tolerance
420 rank. *Forest Ecology and Management* 31: 245–253.

421 Abrams, M. D., M. E. Kubiske, and S. A. Mostoller. 1994. Relating Wet and Dry Year
422 Ecophysiology to Leaf Structure in Contrasting Temperate Tree Species. *Ecology* 75:
423 123–133.

424 Aizen, M. A., and C. Ezcurra. 2008. Do leaf margins of the temperate forest flora of southern
425 South America reflect a warmer past? *Global Ecology and Biogeography* 17: 164–174.

426 Apostol, E. N., A. L. Curtu, L. M. Daia, B. Apostol, C. G. Dinu, and N. Şofletea. 2017. Leaf
427 morphological variability and intraspecific taxonomic units for pedunculate oak and
428 grayish oak (genus *Quercus* L., series *Pedunculatae* Schwz.) in Southern Carpathian
429 Region (Romania). *Science of The Total Environment* 609: 497–505.

430 Auguie, B. 2017. gridExtra: Miscellaneous Functions for 'Grid' Graphics.

431 Bailey, I. W., and E. W. Sinnott. 1915. A Botanical Index of Cretaceous and Tertiary Climates.
432 *Science* 41: 831–834.

433 Bailey, I. W., and E. W. Sinnott. 1916. The Climatic Distribution of Certain Types of Angiosperm
434 Leaves. *American Journal of Botany* 3: 24–39.

435 Baranski, M. J. 1975. An analysis of variation within white oak (*Quercus alba* L.). North Carolina
436 Agricultural Experiment Station, Raleigh.

437 Becker, R. A., A. R. Wilks, R. Brownrigg, T. P. Minka, and A. Deckmyn. 2018. maps: Draw
438 Geographical Maps.

439 Bivand, R. S., E. Pebesma, and V. Gomez-Rubio. 2013. Applied spatial data analysis with R,
440 Second edition. Springer, NY.

441 Blue, M. P., and R. J. Jensen. 1988. Positional and seasonal variation in oak (*Quercus*,
442 Fagaceae) leaf morphology. *American Journal of Botany* 75: 939–947.

443 Bonhomme, V., S. Picq, C. Gaucherel, and J. Claude. 2014. Momocs: Outline Analysis Using R.
444 *Journal of Statistical Software* 56: 1–24.

445 Bragg, J. G., and M. Westoby. 2002. Leaf size and foraging for light in a sclerophyll woodland.
446 *Functional Ecology* 16: 633–639.

447 Bruschi, P., P. Grossoni, and F. Bussotti. 2003. Within- and among-tree variation in leaf
448 morphology of *Quercus petraea* (Matt.) Liebl. natural populations. *Trees* 17: 164–172.

449 Burnham, R. J., and G. S. Tonkovich. 2011. Climate, leaves, and the legacy of two giants. *New*
450 *Phytologist* 190: 514–517.

451 Cavender-Bares, J. 2019. Diversification, adaptation, and community assembly of the American
452 oaks (*Quercus*), a model clade for integrating ecology and evolution. *New Phytologist*
453 221: 669–692.

454 Crampton, J. S. 1995. Elliptic Fourier shape analysis of fossil bivalves: some practical
455 considerations. *Lethaia* 28: 179–186.

456 Ducrey, M. 1992. Variation in leaf morphology and branching pattern of some tropical rain forest
457 species from Guadeloupe (French West Indies) under semi-controlled light conditions.
458 *Annales des Sciences Forestières* 49: 553–570.

459 García-Nogales, A., J. C. Linares, R. G. Laureano, J. I. Seco, and J. Merino. 2016. Range-wide
460 variation in life-history phenotypes: spatiotemporal plasticity across the latitudinal
461 gradient of the evergreen oak *Quercus ilex*. *Journal of Biogeography* 43: 2366–2379.

462 Garner, M., K. K. Pham, A. T. Whittemore, J. Cavender-Bares, P. F. Gugger, P. S. Manos, I. S.
463 Pearse, and A. L. Hipp. 2019. From Manitoba to Texas: A study of the population
464 genetic structure of bur oak (*Quercus macrocarpa*). *International Oaks: The Journal of*
465 *the International Oak Society* 30: 131–138.

466 Genz, A., and F. Bretz. 2009. Computation of Multivariate Normal and t Probabilities. Springer-
467 Verlag, Heidelberg.

468 Genz, A., F. Bretz, T. Miwa, X. Mi, F. Leisch, F. Scheipl, and T. Hothorn. 2019. mvtnorm:
469 Multivariate Normal and t Distributions.

470 Givnish, T. J. 1987. Comparative Studies of Leaf Form: Assessing the Relative Roles of
471 Selective Pressures and Phylogenetic Constraints. *New Phytologist* 106: 131–160.

472 González-Rodríguez, A., D. M. Arias, S. Valencia-Avalos, and K. Oyama. 2004. Morphological
473 and RAPD analysis of hybridization between *Quercus affinis* and *Q. laurina* (Fagaceae),
474 two Mexican red oaks. *American Journal of Botany* 91: 401–409.

475 González-Rodríguez, A., and K. Oyama. 2005. Leaf morphometric variation in *Quercus affinis*
476 and *Q. laurina* (Fagaceae), two hybridizing Mexican red oaks. *Botanical Journal of the*
477 *Linnean Society* 147: 427–435.

478 Greenwood, D. R., P. Wilf, S. L. Wing, and D. C. Christophel. 2004. Paleotemperature
479 Estimation Using Leaf-Margin Analysis: Is Australia Different? *PALAIOS* 19: 129–142.

480 Halloy, S. R. P., and A. F. Mark. 1996. Comparative leaf morphology spectra of plant
481 communities in New Zealand, the Andes and the European Alps. *Journal of the Royal*
482 *Society of New Zealand* 26: 41–78.

483 Hamerlynck, E. P., and A. K. Knapp. 1994. Leaf-level responses to light and temperature in two
484 co-occurring *Quercus* (Fagaceae) species: implications for tree distribution patterns.
485 *Forest Ecology and Management* 68: 149–159.

Haralick, R. M. 1974. A Measure for Circularity of Digital Figures. *IEEE Transactions on Systems, Man, and Cybernetics* SMC-4: 394–396.

Hijmans, R. 2017. raster: Geographic Data Analysis and Modeling. R package version 2.6-7.

Hipp, A. L., P. S. Manos, A. González-Rodríguez, M. Hahn, M. Kaproth, J. D. McVay, S. V. Avalos, and J. Cavender-Bares. 2018. Sympatric parallel diversification of major oak clades in the Americas and the origins of Mexican species diversity. *New Phytologist* 217: 439–452.

Hipp, A. L., A. T. Whittemore, M. Garner, M. Hahn, E. Fitzek, E. Guichoux, J. Cavender-Bares, et al. 2019. Genomic identity of white oak species in an eastern North American syngameon. *Annals of the Missouri Botanical Garden* 104: 455–477.

Hoban, S. 2014. An overview of the utility of population simulation software in molecular ecology. *Molecular Ecology* 23: 2383–2401.

Hoban, S. 2019. New guidance for ex situ gene conservation: Sampling realistic population systems and accounting for collection attrition. *Biological Conservation* 235: 199–208.

Hoban, S., T. Callicrate, J. Clark, S. Deans, M. Dosmann, J. Fant, O. Gailing, et al. 2020. Taxonomic similarity does not predict necessary sample size for ex situ conservation: a comparison among five genera. *Proceedings of the Royal Society B: Biological Sciences* 287: 20200102.

Hoban, S., O. Gaggiotti, and G. Bertorelle. 2013. Sample Planning Optimization Tool for conservation and population Genetics (SPOTG): a software for choosing the appropriate number of markers and samples. *Methods in Ecology and Evolution* 4: 299–303.

Howard, D., R. Preszler, J. Williams, S. Fenchel, and W. Boecklen. 1997. How discrete are oak species? Insights from a hybrid zone between *Quercus grisea* and *Quercus gambelii*. *Evolution* 51: 747–755.

Jensen, R. J. 1990. Detecting shape variation in oak leaf morphology: A comparison of rotational-fit methods. *American Journal of Botany* 77: 1279–1293.

Jensen, R. J., R. Depiero, and B. K. Smith. 1984. Vegetative characters, population variation, and the hybrid origin of *Quercus ellipsoidalis*. *American Midland Naturalist* 111: 364–370.

Kaproth, M. A., and J. Cavender-Bares. 2016. Drought tolerance and climatic distributions of the American oaks. *International Oak Journal* 27: 49–60.

Koenig, W. D., J. M. H. Knops, J. L. Dickinson, and B. Zuckerberg. 2009. Latitudinal decrease in acorn size in bur oak (*Quercus macrocarpa*) is due to environmental constraints, not avian dispersal. *Botany* 87: 349–356.

Kremer, A., J. Dupouey, J. Deans, J. Cottrell, U. Csaikl, R. Finkeldey, S. Espinel, et al. 2002. Leaf morphological differentiation between *Quercus robur* and *Quercus petraea* is stable across western European mixed oak stands. *Annals of Forest Science* 59: 777–787.

523 Li, Y., P. B. Reich, B. Schmid, N. Shrestha, X. Feng, T. Lyu, B. S. Maitner, et al. 2020. Leaf size
524 of woody dicots predicts ecosystem primary productivity. *Ecology Letters* 23: 1003–
525 1013.

526 Little, E. L. 1971. Atlas of United States trees, volume 1, Conifers and important hardwoods.
527 U.S. Dept. of Agriculture, Forest Service, Washington, D.C.□:

528 Little, S. A., S. W. Kembel, and P. Wilf. 2010. Paleotemperature Proxies from Leaf Fossils
529 Reinterpreted in Light of Evolutionary History. *PLOS ONE* 5: e15161.

530 Liu, M., Z. Wang, S. Li, X. Lü, X. Wang, and X. Han. 2017. Changes in specific leaf area of
531 dominant plants in temperate grasslands along a 2500-km transect in northern China.
532 *Scientific Reports* 7: 10780.

533 Marron, N., E. Dreyer, E. Boudouresque, D. Delay, J.-M. Petit, F. M. Delmotte, and F. Brignolas.
534 2003. Impact of successive drought and re-watering cycles on growth and specific leaf
535 area of two Populus × canadensis (Moench) clones, 'Dorskamp' and 'Luisa_Avanzo'. 23:
536 11.

537 McCarthy, D. M., and R. J. Mason-Gamer. 2019. Morphological Variation in North American
538 *Tilia* and Its Value in Species Delineation. *International Journal of Plant Sciences* 181:
539 175–195.

540 McDonald, P. G., C. R. Fonseca, J. M. Overton, and M. Westoby. 2003. Leaf-size divergence
541 along rainfall and soil-nutrient gradients: is the method of size reduction common among
542 clades? *Functional Ecology* 17: 50–57.

543 McKee, M. L., D. L. Royer, and H. M. Poulos. 2019. Experimental evidence for species-
544 dependent responses in leaf shape to temperature: Implications for paleoclimate
545 inference. *PLOS ONE* 14: e0218884.

546 McKee, M., and D. L. Royer. 2017. How Does Temperature Impact Leaf Size and Shape in Four
547 Woody Dicot Species? Testing the Assumptions of Leaf Physiognomy-Climate Models.
548 *AGU Fall Meeting Abstracts* 11.

549 Minchin, P. R. 1987. An evaluation of the relative robustness of techniques for ecological
550 ordination. *Vegetatio* 69: 89–107.

551 Moles, A. T., S. E. Perkins, S. W. Laffan, H. Flores-Moreno, M. Awasthy, M. L. Tindall, L. Sack,
552 et al. 2014. Which is a better predictor of plant traits: temperature or precipitation?
553 *Journal of Vegetation Science* 25: 1167–1180.

554 Mooney, H. A., and E. L. Dunn. 1970. Convergent Evolution of Mediterranean-Climate
555 Evergreen Sclerophyll Shrubs. *Evolution* 24: 292–303.

556 Oksanen, J., F. G. Blanchet, M. Friendly, R. Kindt, P. Legendre, D. McGlinn, P. R. Minchin, et
557 al. 2017. vegan: Community Ecology Package. R package version 2.4-5.

558 Pebesma, E. J., and R. S. Bivand. 2005. Classes and methods for spatial data in R. *R News* 5:
559 9–13.

Peppe, D. J., D. L. Royer, B. Cariglino, S. Y. Oliver, S. Newman, E. Leight, G. Enikolopov, et al. 2011. Sensitivity of leaf size and shape to climate: global patterns and paleoclimatic applications. *New Phytologist* 190: 724–739.

R Core Team. 2018. R: A language and environment for statistical computing, version 3.4.4. R Foundation for Statistical Computing, Vienna.

Ramírez-Valiente, J. A., and J. Cavender-Bares. 2017. Evolutionary trade-offs between drought resistance mechanisms across a precipitation gradient in a seasonally dry tropical oak (*Quercus oleoides*). *Tree Physiology*: 1–13.

Ramírez-Valiente, J. A., A. Center, J. Sparks, K. Sparks, J. Etterson, T. Longwell, G. Pilz, and J. Cavender-Bares. 2017. Population-level differentiation in growth rates and leaf traits in seedlings of the neotropical live oak *Quercus oleoides* grown under natural and manipulated precipitation regimes. *Frontiers in Plant Science* 8.

Ramírez-Valiente, J. A., R. López, A. L. Hipp, and I. Aranda. 2020. Correlated evolution of morphology, gas exchange, growth rates and hydraulics as a response to precipitation and temperature regimes in oaks (*Quercus*). *New Phytologist* 227: 794–809.

Rodríguez-Correa, H., K. Oyama, I. MacGregor-Fors, and A. González-Rodríguez. 2015. How are oaks distributed in the neotropics? A perspective from species turnover, areas of endemism, and climatic niches. *International Journal of Plant Sciences* 176: 222–231.

Rosin, P. L. 2005. Computing global shape measures. Handbook of Pattern Recognition and Computer Vision, 177–196. WORLD SCIENTIFIC.

Royer, D. L., J. C. McElwain, J. M. Adams, and P. Wilf. 2008. Sensitivity of leaf size and shape to climate within *Acer rubrum* and *Quercus kelloggii*. *New Phytologist* 179: 808–817.

Royer, D. L., and P. Wilf. 2006. Why Do Toothed Leaves Correlate with Cold Climates? Gas Exchange at Leaf Margins Provides New Insights into a Classic Paleotemperature Proxy. *International Journal of Plant Sciences* 167: 11–18.

Royer, D. L., P. Wilf, D. A. Janesko, E. A. Kowalski, and D. L. Dilcher. 2005. Correlations of climate and plant ecology to leaf size and shape: potential proxies for the fossil record. *American Journal of Botany* 92: 1141–1151.

Schmerler, S. B., W. L. Clement, J. M. Beaulieu, D. S. Chatelet, L. Sack, M. J. Donoghue, and E. J. Edwards. 2012. Evolution of leaf form correlates with tropical-temperate transitions in Viburnum (Adoxaceae). *Proceedings of the Royal Society B: Biological Sciences* 279: 3905–3913.

Schnabel, A., and J. L. Hamrick. 1990. Comparative Analysis of Population Genetic Structure in Quercus macrocarpa and *Q. gambelii* (Fagaceae). *Systematic Botany* 15: 240–251.

Schneider, C. A., W. S. Rasband, and K. W. Eliceiri. 2012. NIH Image to ImageJ: 25 years of image analysis. *Nature Methods* 9: 671–675.

Sokal, R. R., T. J. Crovello, and R. S. Unnasch. 1986. Geographic Variation of Vegetative Characters of Populus deltoides. *Systematic Botany* 11: 419–432.

598 Stein, J., D. Binion, and R. Acciavatti. 2003. Field Guide to Native Oak Species of Eastern North
599 America (FHTET-2003-01). United States Department of Agriculture Forest Service,
600 Forest Health Technology Enterprise Team, Morgantown.

601 Tracey, S. R., J. M. Lyle, and G. Duhamel. 2006. Application of elliptical Fourier analysis of
602 otolith form as a tool for stock identification. *Fisheries Research* 77: 138–147.

603 Walls, R. L. 2011. Angiosperm leaf vein patterns are linked to leaf functions in a global-scale
604 data set. *American Journal of Botany* 98: 244–253.

605 Wickham, H. 2009. ggplot2: Elegant Graphics for Data Analysis. Springer-Verlag, New York.

606 Wright, I. J., N. Dong, V. Maire, I. C. Prentice, M. Westoby, S. Díaz, R. V. Gallagher, et al. 2017.
607 Global climatic drivers of leaf size. *Science* 357: 917–921.

608 Wright, I. J., P. B. Reich, M. Westoby, D. D. Ackerly, Z. Baruch, F. Bongers, J. Cavender-Bares,
609 et al. 2004. The worldwide leaf economics spectrum. *Nature* 428: 821–827.

610

611 **Table 1. Sampling localities, Bioclim values for each site, number of leaves collected per**

612 **tree.** Only leaves used for statistical analysis are counted. Broken or incomplete leaves were

613 eliminated from statistical analysis. Abbreviations: Bio1 = mean annual temperature (in degrees

614 C); Bio12 = mean annual precipitation (in mm).

Site	Bio1, Bio12	Tree	Latitude	Longitude	Lvs
Whiteshell Provincial Park	2.07℃, 566 mm	MB-SD004	49.4249	-95.1436	8
		MB-SD005	49.71279	-95.2444	8
		MB-MG513	49.71209	-95.24496	8
Spruce Woods Provincial Park	2.50℃, 460 mm	MB-MG516	49.76104	-99.15971	8
		MB-MG517	49.76095	-99.15983	8
		MB-MG518	49.76061	-99.15928	8
Assiniboine Forest	2.10℃, 519 mm	MB-MG528	49.85778	-97.24848	8
		MB-MG529	49.85423	-97.2482	8
		MB-MG530	49.85392	-97.24828	8
University of Minnesota	7.10℃, 738 mm	MN-MG788	44.97882	-93.23768	8
Campus		MN-MG789	44.97739	-93.23761	8
		MN-MG790	44.97771	-93.23801	7
Cherokee Park Trail	9.20℃, 879 mm	IA-MG243	41.97454	-91.72161	8
		IA-MG244	41.97367	-91.72547	8
		IA-MG245	41.97362	-91.72565	6
Morton Arboretum	9.50℃, 932 mm	IL-SF001	41.81696	-88.0808	8
		IL-SF002	41.81331	-88.08266	8
		IL-SF003	41.81588	-88.07994	8
Prairie Moon Nursery	6.80℃, 837 mm	MN-SD001	43.89117	-91.64684	8
		MN-SD002	43.89804	-91.648	8
		MN-SD003	43.89088	-91.64689	2
Burr Oak Woods	9.80℃, 943 mm	IN-MG631	41.53273	-87.2948	8
		IN-MG636	41.5345	-87.29279	8
		IN-MG638	41.53253	-87.29661	8
Red Rock Canyon State Park	15.3℃, 756 mm	OK-MG369	35.43874	-98.35495	8
		OK-MG370	35.43851	-98.35503	8
		OK-MG371	35.43854	-98.35497	8
Mohawk Park	15.3℃, 987	OK-MG347	36.21066	-95.89467	8

	mm				
		OK-MG349	36.2204	-95.89845	8
		OK-MG350	36.22064	-95.89877	8
Tallgrass Prairie Preserve	14.3℃, 939 mm	OK-MG282	36.84504	-96.42526	8
		OK-MG283	36.84485	-96.42479	2
		OK-MG284	36.84501	-96.42553	3
Buttin Rock Access	13.1℃, 1121 mm	MO-MG402	37.15687	-91.36471	8
		MO-MG403	37.15686	-91.36501	8
		MO-MG404	37.15726	-91.36518	8

615

616 **Table 2. Descriptions of the leaf traits measured**

	Leaf measurements	
Trait	**Abbreviation**	**Definition**
Blade length (mm)	bladeL	Straight line distance measured from intersection of leaf and petiole to tip of the leaf at its point of intersection with the midvein
Blade width (mm)	bladeW	The longest possible perpendicular line drawn from one edge of the blade to the other; vein position used to identify the leaves opposite one another
Width of blade between deepest pair of sinuses (mm)	sinusMinL	The shortest distance that separates the deepest sinus from its corresponding sinus. (The deepest sinus is defined as the sinus that has the longest distance from the most interior point of the sinus to the line that connects the two most exterior points of that sinus)
Width of blade between sinuses just above the deepest pair (mm)	sinusNextL	The width between the sinuses that are immediately distal to the deepest sinuses (as defined in sinusMinL)
Petiole length (mm)	petioleL	Measured from the base of the blade as defined by bladeL to the base of the petiole, defined as the line of intersection between petiole and branch, upper surface of the petiole
Petiole width (mm)	petioleW	Measured at the point of intersection between the blade and the petiole, where blade is not visible
Length of lamina from base to widest point (mm)	bladeLtoWidestPoint	Measured from the base of the blade to the point of intersection between the midvein and the line used to measure leaf blade width
Blade base angle (degrees)	bladeBaseAngle	Measured using the lines that define the widest angle between the base and either edge of the leaf
Total length (mm)	BL.PL	Total length is the blade length added to the petiole length
Leaf area (mm^2)	Area	Calculated in imageJ.

Ratios		
Petiole length / Total length	PL.TL	The petiole length divided by the total length
Sinus ratio	SinusRatio	The width of the blade between the deepest pair of sinuses divided by the width of the blade between the pair of sinuses just above the deepest pair
Blade length/ Blade width	BL.BW	The blade length divided by the blade width
Petiole length / Petiole width	PL.PW	The petiole length divided by the petiole width
Blade length / Blade length to widest point	BL.BLWP	The blade length divided by the length of the blade from the base to the widest point
Ratio of Leaf size to petiole length	BL.BW.over.PL.PW	The blade length divided by the blade width divided by the petiole length divided by the petiole width
Specific leaf area	SLA	Leaf area divided by the mass of the leaf
Lobedness	sinus.v.width	The width of the blade between the deepest pair of sinuses divided by the blade width

617

618

619

620 **Table 3. Simple and multiple regressions for all leaf traits.** The columns for Blade length and
621 Latitude represent the regression coefficient and p-value for a multiple regression with each leaf
622 trait regressed against Blade length and Latitude. Note that after Bonferroni correction for
623 multiple tests, only the regression of blade length on latitude + petiole width is significant; and
624 for that multiple regression, only the coefficient for latitude is significant

Leaf trait	p-value	r^2	Blade length	Latitude	R^2
bladeL	0.012	0.486		-0.697, p = 0.012	0.486
bladeW	0.014	0.469	0.926, p < .001	-0.039, p = 0.780	0.911
sinusMinL	0.208	0.153	-0.069, p = 0.874	0.343, p = 0.443	0.156
sinusNextL	0.492	0.048	0.966, p = 0.014	0.893, p = 0.021	0.528
petioleL	0.262	0.124	0.812, p = 0.041	0.214, p = 0.546	0.463
petioleW	p < 0.001	0.692	0.119, p = 0.649	-0.749, p = 0.017	0.699
bladeLtoWidestPoint	0.011	0.494	0.920, p < .001	-0.062, p = 0.630	0.929
bladeBaseAngle	0.151	0.195	-0.363, p = 0.386	-0.695, p = 0.116	0.263
TotalL.PL.BL	0.019	0.438	1.03, p < 0.001	0.052, p = 0.459	0.979
Area	0.014	0.469	0.949, p <0 .001	-0.024, p = 0.847	0.933
SLA	0.015	0.466	0.438, p = 0.188	0.987, p = 0.011	0.564
PL.TL	0.945	r^2 < 0.001	0.347, p = 0.461	0.264, p = 0.572	0.062
SinusRatio	0.425	0.065	-0.253, p = 0.580	0.078, p = 0.864	0.098
BL.BW	0.313	0.101	-0.367, p = 0.408	0.062, p = 0.886	0.171
BL.BLWP	0.834	0.005	0.183, p = 0.699	0.196, p = 0.680	0.022
sinus.v.width	0.024	0.415	-0.551, p = 0.103	0.259, p = 0.415	0.571
sinus.v.width (no spruce woods)	0.054	0.352	-0.296, p = 0.152	0.163, p = 0.391	0.507

625

626

627 **Table 4. ANOVA for bladeL, SLA, PC1, PC2**

Response		Df	Sum of Squares	Mean Square	F-value	Pr(>F)
bladeL	site	11	177345	16122.3	38.9996	< 2.2e-16
	tree	24	83159	3465.0	8.3817	< 2.2e-16
	residuals	236	97562	413.4		
SLA	site	11	1017054857	92459532	30.3766	< 2.2e-16
	tree	24	703085034	29295210	9.6246	< 2.2e-16
	residuals	236	718331913	3043779		
PC1	site	11	984.70	89.519	41.7620	<2.2e-16
	tree	24	300.10	12.504	5.8335	8.101e-14
	residuals	236	505.88	2.144		
PC2	site	11	400.34	36.394	34.042	<2.2e-16
	tree	24	318.70	13.279	12.421	<2.2e-16
	residuals	236	252.30	1.069		

628

629

630

631 **FIGURE LEGENDS**

632

633 Figure 1. Locations of sampling sites for this study as well as mean annual temperature across
634 the bur oak range. WorldClim temperature data are scaled to a factor of 10. Specific information
635 about site, name, location, and number of samples collected can be found in Table 1.

636

637 Figure 2. Leaf trait measurements used in this study. All measurements used in this study were
638 linear measurements or ratios of linear measurements, plus one angle. Details and definitions are
639 found in Table 4.

640

641 Figure 3. Simple regressions of traits and environment that are significant at the 0.05 level. P-
642 values are not corrected for multiple tests; a total of seventeen regressions were performed
643 (Table 3).

644

645 Figure 4. Simple regressions of circularity on latitude.

646

647 Figure 5. Regressions of bioclim variables on latitude. Latitude shows up as the strongest single
648 predictor of leaf morphology in the current study, as it integrates over both day length and
649 several aspects of climate: bio 1 (mean annual temperature), bio 12 (mean annual precipitation),
650 bio 4 (mean temperature seasonality).

651

652 Figure 6. Sampling simulations. Simulated sampling strategies accounted for covariance among
653 traits within leaves; among leaves on trees within sites; and among trees within sites. Here, two
654 estimates of power are reported: the number of groups of sites recognized as distinct from each
655 other using Tukey's HSD at $\alpha = 0.05$; and the probability of recognizing at least 50% of sites as
656 distinct from each other. colors scale from darker as a higher number of groups are recognized,
657 lighter as fewer are. Simulated numbers of sites distinguished (left panel) and probabilities of
658 distinguishing at least 50% of simulated sites (right panel) are reported in each cell of the
659 simulation.
660
661 Supplemental Figure S1. Biplots of all simple regressions performed, whether significant or not
662 Supplemental Figure S2. PCA based on eFourier analysis of leaf outlines.
663 Supplemental Figure S3. Non-metric multidimensional scaling ordination of PCA on leaf
664 measurements

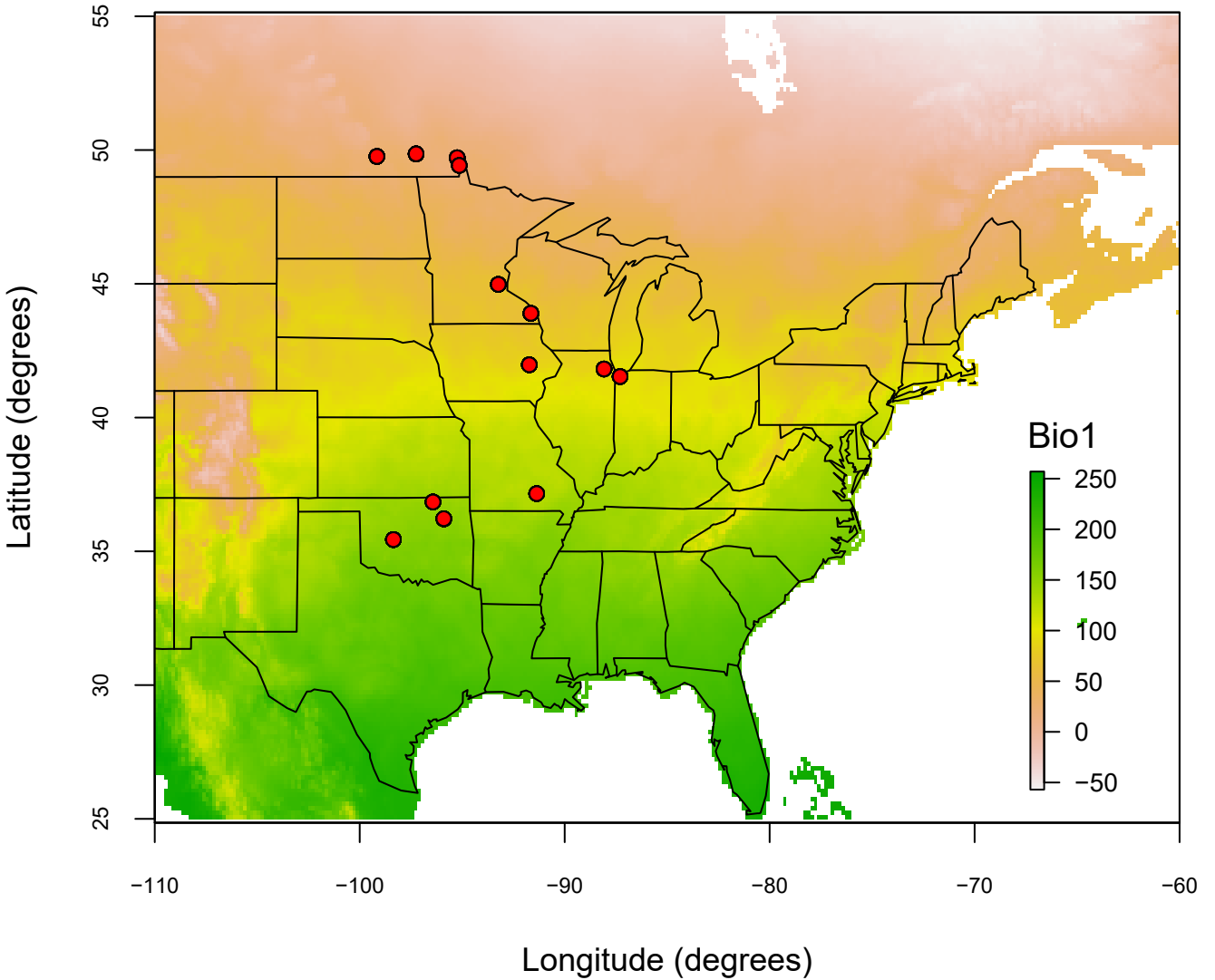
Latitude (degrees)
55
50
45
40
35
30
25
−110
−100
−90
−80
−70
−60
Longitude (degrees)
Bio1
250
200
150
100
50
0
−50

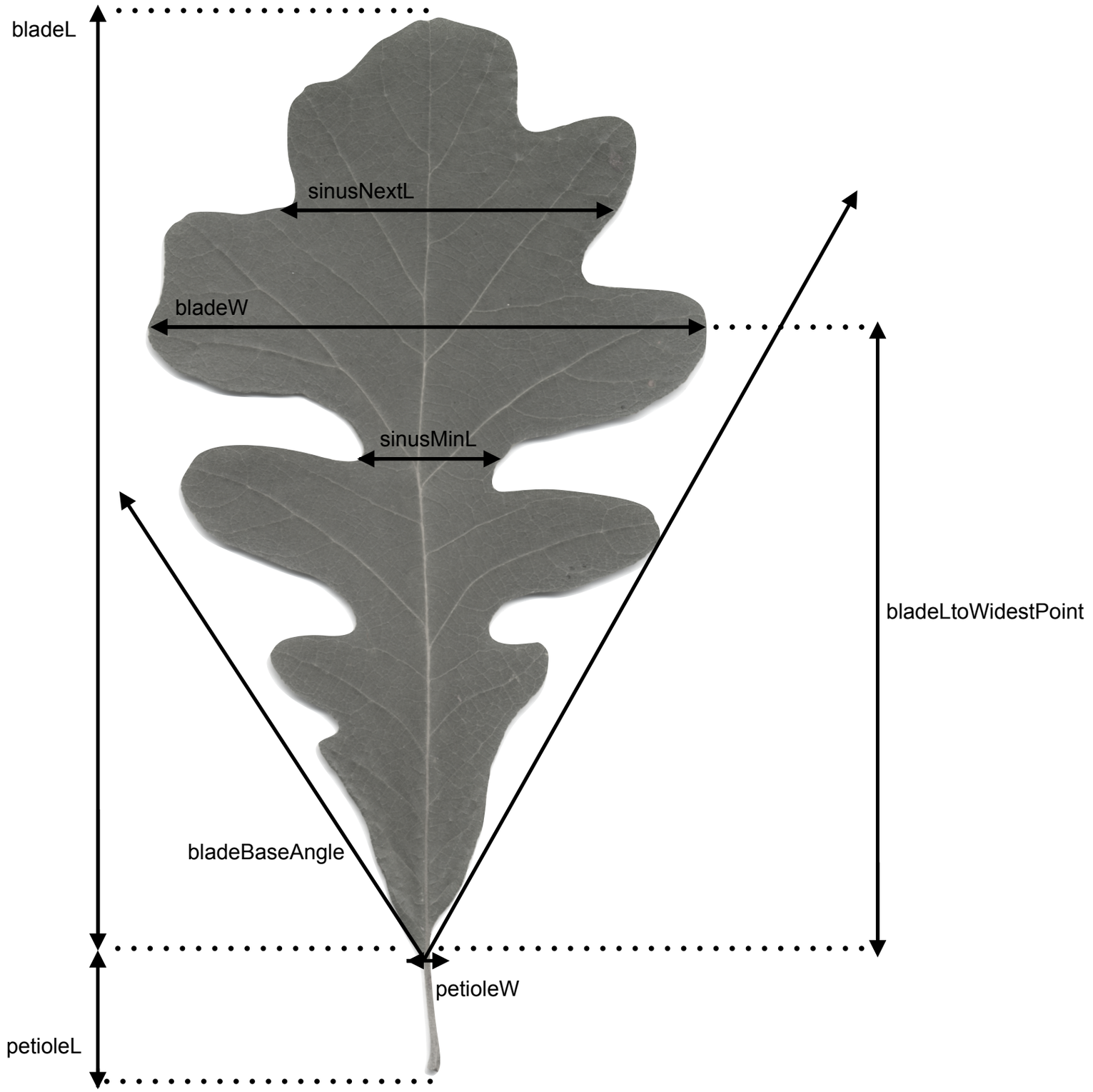

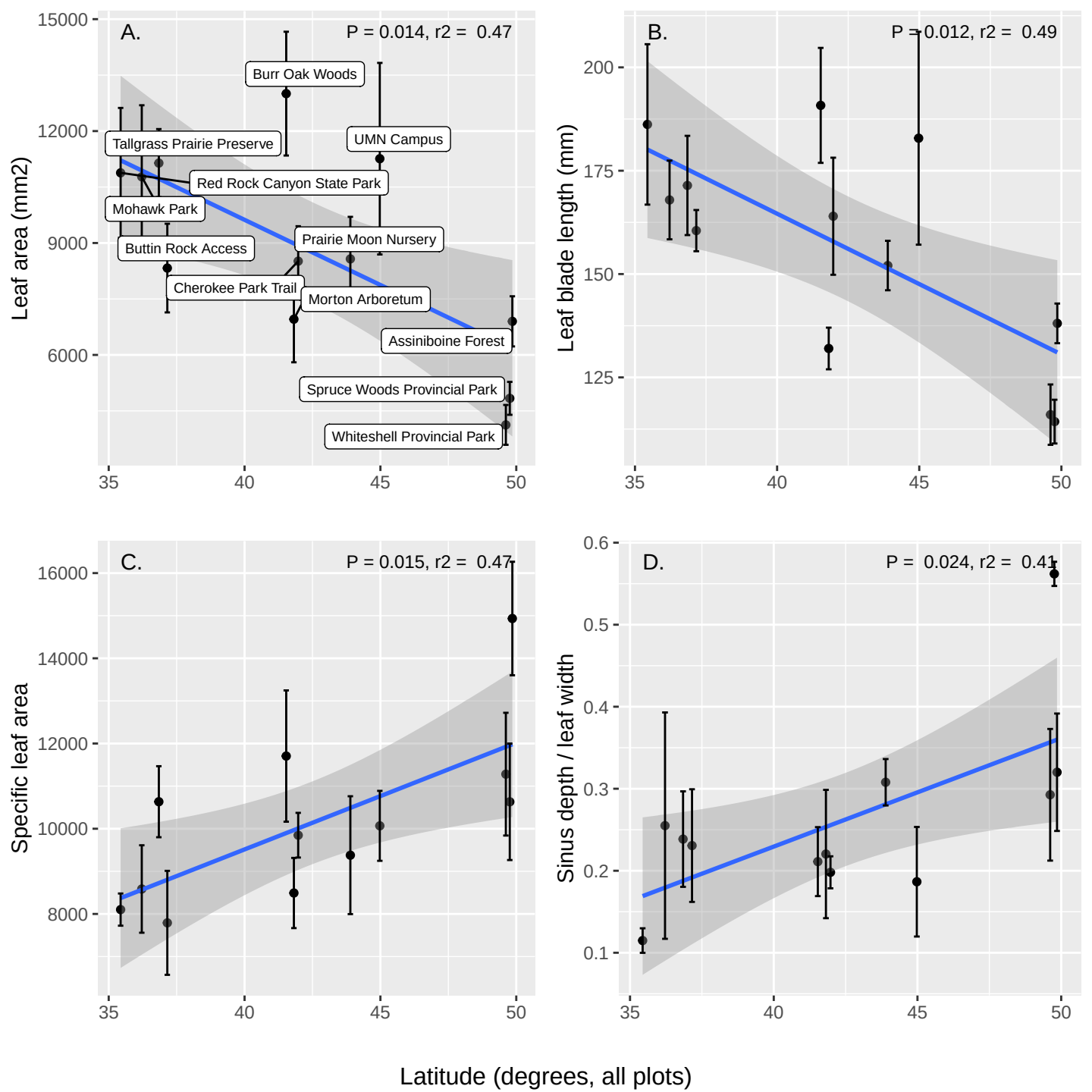
A.
P = 0.014, r2 = 0.47
Leaf area (mm2)
15000
12000
9000
6000
Burr Oak Woods
Tallgrass Prairie Preserve
UMN Campus
Red Rock Canyon State Park
Mohawk Park
Buttin Rock Access
Prairie Moon Nursery
Cherokee Park Trail
Morton Arboretum
Assiniboine Forest
Spruce Woods Provincial Park
Whiteshell Provincial Park
35
40
45
50
B.
P = 0.012, r2 = 0.49
Leaf blade length (mm)
200
175
150
125
C.
P = 0.015, r2 = 0.47
Specific leaf area
16000
14000
12000
10000
8000
D.
P = 0.024, r2 = 0.41
Sinus depth / leaf width
0.6
0.5
0.4
0.3
0.2
0.1
Latitude (degrees, all plots)

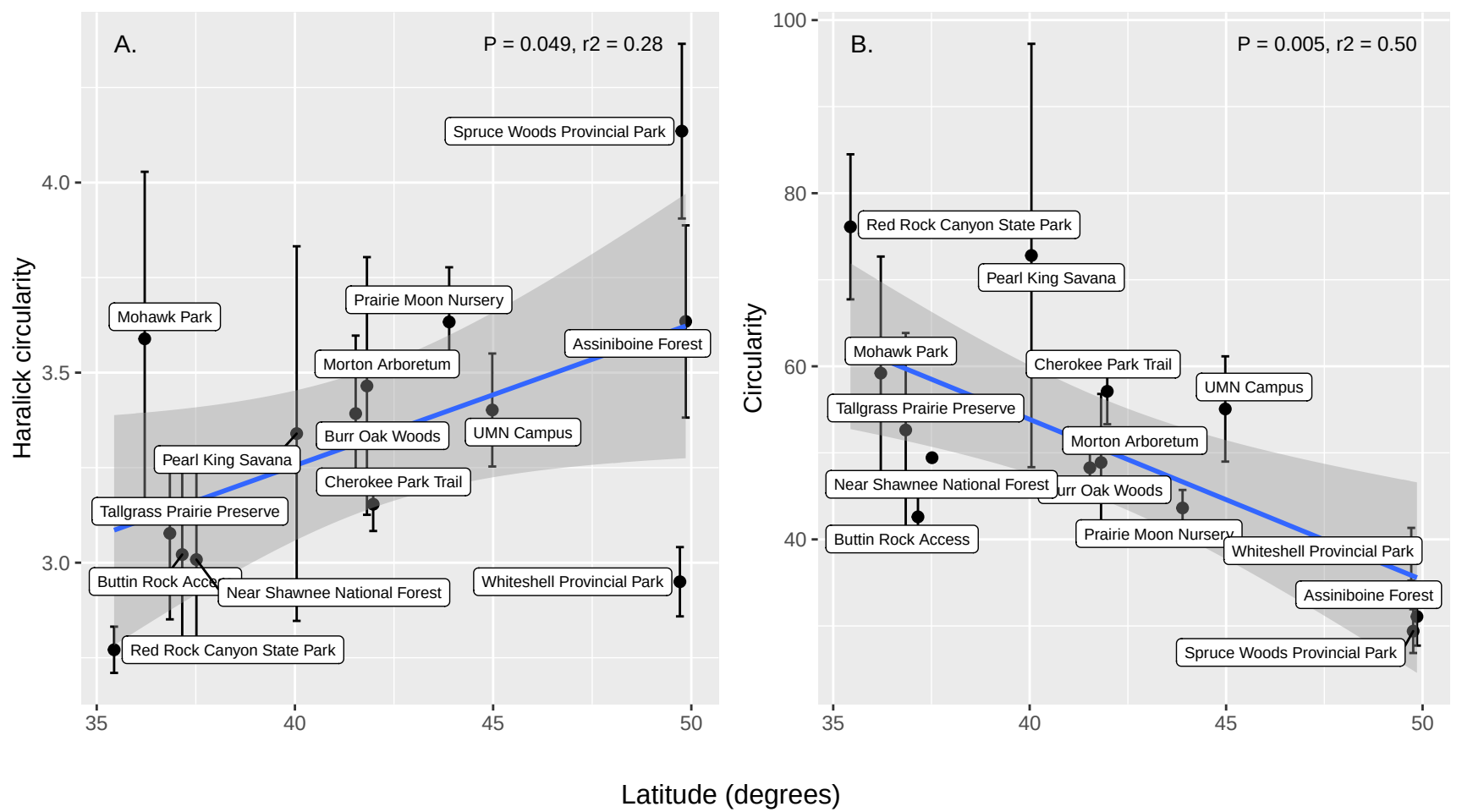
A.
P = 0.049, r2 = 0.28
Haralick circularity
4.0
3.5
3.0
Spruce Woods Provincial Park
Mohawk Park
Prairie Moon Nursery
Assiniboine Forest
Morton Arboretum
Burr Oak Woods
UMN Campus
Pearl King Savana
Cherokee Park Trail
Tallgrass Prairie Preserve
Buttin Rock Acce
Near Shawnee National Forest
Whiteshell Provincial Park
Red Rock Canyon State Park
35
40
45
50
B.
P = 0.005, r2 = 0.50
Circularity
100
80
60
40
Red Rock Canyon State Park
Pearl King Savana
Mohawk Park
Cherokee Park Trail
UMN Campus
Tallgrass Prairie Preserve
Morton Arboretum
Near Shawnee National Forest
urr Oak Woods
Buttin Rock Access
Prairie Moon Nursery
Whiteshell Provincial Park
Assiniboine Forest
Spruce Woods Provincial Park
35
40
45
50
Latitude (degrees)

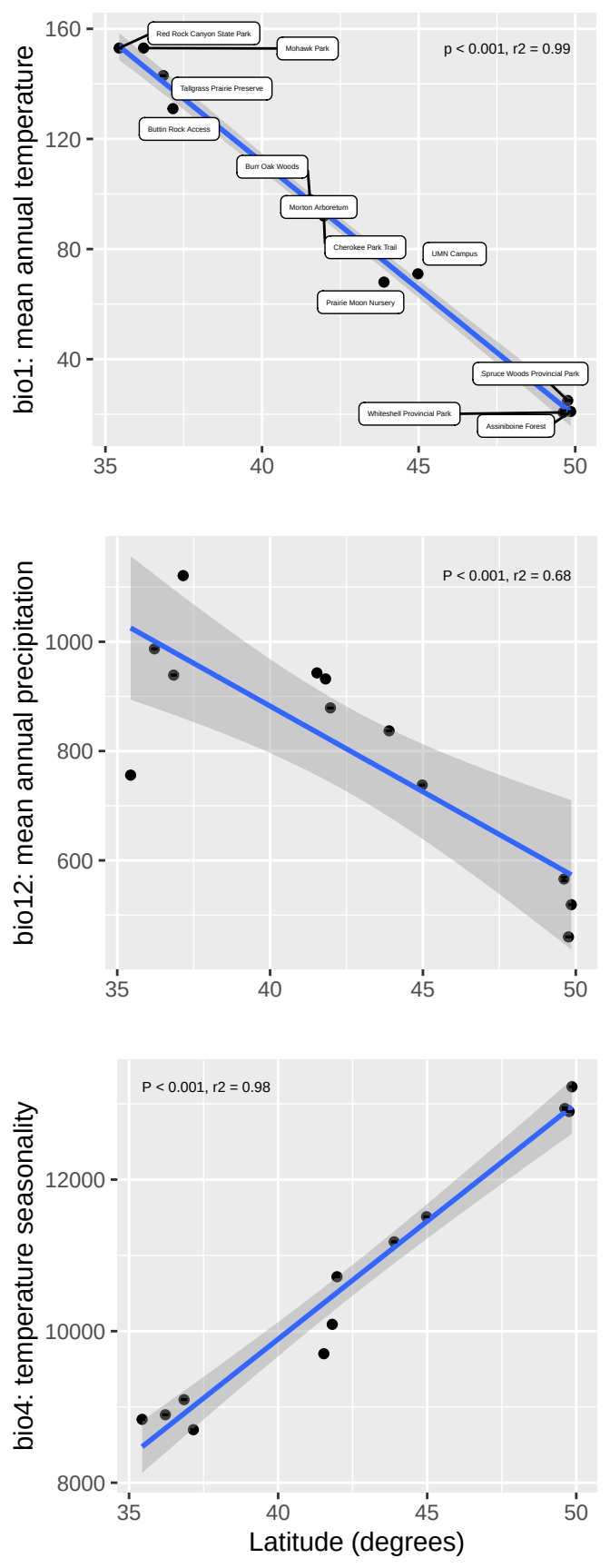
bio1: mean annual temperature
p < 0.001, r2 = 0.99
Red Rock Canyon State Park
Mohawk Park
Tallgrass Prairie Preserve
Buttin Rock Access
Burr Oak Woods
Morton Arboretum
Cherokee Park Trail
UMN Campus
Prairie Moon Nursery
Spruce Woods Provincial Park
Whiteshell Provincial Park
Assiniboine Forest
160
120
80
40
35
40
45
50
bio12: mean annual precipitation
P < 0.001, r2 = 0.68
1000
800
600
bio4: temperature seasonality
P < 0.001, r2 = 0.98
12000
10000
8000
Latitude (degrees)


Mean groups recognized out of 20 populations
Probability of recognizing 50 percent of populations
Number of trees per site
Number of leaves per tree
12 11 10 9 8 7 6 5 4 3
3 4 5 6 7 8 9 10 11 12
9.01 9.26 9.31 9.64 9.93 10.02 9.77 10.31 10.41 10.15
8.76 9.08 9.42 9.49 9.44 9.92 10 10.1 10.41 10.17
8.86 9.07 9.46 9.4 9.73 9.84 9.76 10.22 10.21 10.17
8.65 8.93 9.01 9.44 9.57 9.66 9.66 9.73 9.97 9.92
7.96 8.64 8.66 9.37 9.76 9.85 9.83 9.93 9.62 9.83
7.7 8.5 8.81 9.08 9.47 9.48 9.66 9.7 10.07 9.56
7.72 8.56 8.51 9.01 9.27 9.12 9.68 9.84 9.84 9.82
7.25 7.99 8.66 8.43 8.8 9.09 9.08 9.27 9.6 9.61
7.06 7.56 8.25 8.29 8.77 8.82 8.9 9.42 9.07 9.34
6.49 7.13 7.93 8.18 8.44 8.82 9.06 8.86 9.19 9.05
0.39 0.44 0.47 0.56 0.66 0.64 0.56 0.71 0.7 0.66
0.31 0.4 0.5 0.51 0.46 0.61 0.61 0.64 0.69 0.65
0.31 0.43 0.55 0.41 0.58 0.57 0.58 0.67 0.63 0.62
0.32 0.35 0.41 0.5 0.53 0.59 0.52 0.53 0.58 0.62
0.17 0.28 0.33 0.47 0.55 0.58 0.59 0.61 0.52 0.58
0.09 0.25 0.32 0.36 0.49 0.55 0.59 0.56 0.62 0.52
0.14 0.2 0.28 0.33 0.47 0.38 0.55 0.58 0.57 0.58
0.07 0.15 0.29 0.24 0.31 0.36 0.47 0.42 0.51 0.57
0.05 0.09 0.22 0.27 0.32 0.34 0.34 0.48 0.42 0.46
0.01 0.04 0.15 0.15 0.21 0.38 0.35 0.37 0.43 0.35